Implementation of the photonic time-stretch concept using an incoherent pulsed light source

Bo Li,[1,2,*] Shuqin Lou,[2] and José Azaña[1]

[1]Institut National de la Recherche Scientifique—Energie, Matériaux et Télécommunications, Montréal, Québec H5A 1K6, Canada

[2]School of Electronic and Information Engineering, Beijing Jiaotong University, Beijing 100044, China

*Corresponding author: liboresearch@gmail.com

Received 17 December 2014; revised 26 February 2015; accepted 28 February 2015; posted 2 March 2015 (Doc. ID 230808); published 25 March 2015

We propose a new technique to realize photonic time stretching of radio-frequency (RF) signals by using a time-gated (pulsed) incoherent-light source. The proposed system provides similar performance specifications (stretch factor, temporal aperture, and resolution) to those of a conventional coherent system but using a temporal gating process that is significantly longer than the transform-limited pulse duration of the equivalent coherent configuration. We experimentally demonstrate temporal magnification and compression of high-speed RF signals, with time-stretch factors ranging from 0.65 to 8.66, using a broadband (11.6 nm) incoherent-light source temporally gated over ~163 ps. In one of the reported experiments, we achieve a resolution of ~67.5 ps over a temporal aperture of ~23 ns, representing a time–bandwidth product of >340.

OCIS codes: (070.1170) Analog optical signal processing; (110.6915) Time imaging; (320.7085) Ultrafast information processing.

http://dx.doi.org/10.1364/AO.54.002757

1. Introduction

Digital signal processing can support ultrahigh-speed data processing and excellent reconfigurability. To translate the analog signals, which are common in nature, to digital signals, an analog-to-digital converter is required. However, the realization of ultrahigh-speed (or ultrawide-bandwidth) analog-to-digital converters has been recognized as a key bottleneck in modern high-performance communication and radar systems [1–3]. The photonic time-stretch concept has proven to be a very effective approach to address this problem [1–6]. In a time-stretch system, the signal is temporally stretched while keeping its original time shape prior to digitization so that the effective sampling rate and bandwidth of the analog-to-digital convertor are improved in proportion to the time-stretch factor. Additionally, the time-stretch technology has also been used to realize other important applications, for instance, high-throughput single-shot spectroscopy [7].

A main limitation of a time-stretch system is the realization of a linearly chirped optical pulse, which is conventionally obtained by dispersing the output of a coherent ultrafast optical pulsed source, e.g., a femtosecond mode-locked laser [2–7]. However, relatively complex and costly techniques (e.g., mode locking) are required to be able to produce coherent optical pulses with wavelength bandwidths extending even over a few nanometers. Compared to a coherent-light source, it is generally more practical and simpler to produce incoherent light with large wavelength (frequency) bandwidths. In the latter case, phase-locking mechanisms are not needed. In this work, we propose and experimentally demonstrate a novel photonic time-stretch system based on an incoherent-light source. The scheme is based on the use of an incoherent pulsed light source, which is implemented by modulating broadband incoherent light with a short temporal gate. Note that incoherent-light temporal stretching has recently been

1559-128X/15/102757-05$15.00/0

proposed using a time-domain equivalent of a spatial pinhole [8]. The new scheme proposed here is essentially based on exchanging the short temporal gating process (time-domain pinhole) and signal modulation process in the original temporal pinhole imaging system. This translates into a scheme that resembles much more closely the conventional coherent photonic time-stretch configuration, where the original coherent pulsed (mode-locked) optical source is simply substituted by an incoherent pulsed light source. Notice that though related, photonic time-stretch and temporal imaging are different concepts [4]; for example, the temporal resolution and magnification factors of these two systems are different. We show here the implementation of the photonic time-stretch concept using an incoherent-light pulsed light source. Another key finding of our work is that the light source bandwidth impacts the system performance (particularly, the temporal aperture) in a very similar fashion to that of a coherent time-stretch system; however, the temporal gate can be much longer than the coherence time of the light source, or the transform-limited duration of the equivalent coherent pulsed source, while still achieving similar performance in terms of temporal resolution. This points again to the fact that phase locking over the entire source bandwidth is not required in the system.

2. Principles

An illustration of the proposed incoherent photonic time-stretch scheme is shown in Fig. 1. Compared to its coherent counterpart, the scheme employs a broadband incoherent pulsed source. The incoherent pulsed source is achieved by short temporal gating of a broadband incoherent-light source, which is assumed to exhibit a uniform energy spectrum over a broad bandwidth. To be consistent with previous terminology, the short temporal gating process will be referred to as a "temporal pinhole". Temporal stretching of the intensity waveform under test is achieved through a concatenation of time-to-frequency and subsequent frequency-to-time mapping processes. In particular, the broadband incoherent pulse is first dispersed by a dispersive element, which provides a group-delay dispersion of $\ddot{\Phi}_1$. As such, an averaged linear frequency chirp is induced in the time domain.

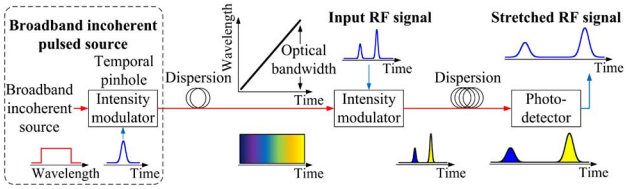

Fig. 1. Diagram of an incoherent photonic time-stretch scheme. Similar to its coherent counterpart, the scheme consists of two main steps, which are time-to-frequency mapping of the input intensity waveform, implemented at the output of the second intensity modulator, and frequency-to-time mapping, which is induced by the second dispersion, respectively. All waveforms and spectra, and the instantaneous wavelength, are averaged profiles.

This is followed by a second temporal intensity modulation process with the input radio-frequency (RF) signal to be processed; the RF temporal waveform is mapped along the frequency domain (time-to-frequency mapping) as a result of the optical pulse linear frequency chirp. The resulting modulated light is finally dispersed by the second dispersive element with a group-delay dispersion of $\ddot{\Phi}_2$, effectively mapping the modulated light spectrum along the time domain. This results in the anticipated temporal stretching process of the original RF signal.

It can be shown that the temporal impulse response function of the proposed incoherent photonic time-stretch system is mathematically described by the following expression:

$$\langle I_{\text{out}}(\tau)\rangle \propto I_{\text{pinhole}}\left(-\frac{\ddot{\Phi}_1}{\ddot{\Phi}_2}\tau\right) \otimes I_{\text{signal}}\left(\frac{\ddot{\Phi}_1}{\ddot{\Phi}_1+\ddot{\Phi}_2}\tau\right), \quad (1)$$

where $I_{\text{pinhole}}(\tau)$, $I_{\text{signal}}(\tau)$, and $I_{\text{out}}(\tau)$ are the temporal intensity profiles of the temporal pinhole, the input signal to be processed, and the system output, respectively; τ is the normalized time so that the average group delay in each of the constituting elements is ignored; and $\langle\cdot\rangle$ denotes averaging over multiple realizations. It is important to note that Eq. (1) is valid as long as the angular frequency bandwidth of the input signal $\Delta\omega_{\text{sig}}$ is sufficiency small, so that

$$\left|-\frac{\ddot{\Phi}_1\ddot{\Phi}_2}{8(\ddot{\Phi}_1+\ddot{\Phi}_2)}\Delta\omega_{\text{sig}}^2\right| \ll \pi. \quad (2)$$

As shown in Eq. (1), the averaged temporal intensity profile at the system output is a temporally stretched replica of the input temporal waveform, where the stretch factor is given by $M = 1 + (\ddot{\Phi}_2/\ddot{\Phi}_1)$. In practice, the magnitude of M can be fixed to be lower than 1, leading to a temporally compressed replica of the input, or higher than 1, thus implementing temporal magnification. Notice that the condition in Eq. (2) is actually a constraint on the maximum frequency bandwidth of the input signal that can be accurately processed, effectively limiting the system temporal resolution. This same condition applies to a conventional coherent time-stretch system [4,5]. Additionally, in an incoherent time-stretch system, the output temporal image is convolved with the scaled temporal intensity profile of the pinhole, as shown by Eq. (1). This imposes an additional lower bound on the temporal resolution; in particular, the minimum output temporal resolution is $\delta\tau_{\text{out}} = |\ddot{\Phi}_2/\ddot{\Phi}_1|\Delta T_P$, which is estimated as the full width at half-maximum (FWHM) of the intensity profile $I_{\text{pinhole}}[-(\ddot{\Phi}_1/\ddot{\Phi}_2)\tau]$ in Eq. (1), where the pinhole has a Gaussian profile, $I_{\text{pinhole}}(\tau) = |\exp[-2\ln 2(\tau/\Delta T_P)^2]|^2$. The corresponding minimum input resolution can be obtained by scaling through the temporal stretch factor:

$$\delta\tau_{\text{in}} = \left|\frac{\ddot{\Phi}_2}{\ddot{\Phi}_1+\ddot{\Phi}_2}\right|\Delta T_P. \quad (3)$$

To optimize the resolution of the incoherent system, the temporal pinhole duration should be made sufficiently short so that the input resolution bound in Eq. (3) is equal to or higher than the "coherent" resolution dictated by Eq. (2). Notice also that the resolution bound in Eq. (3) is directly limited by the temporal pinhole duration for large stretch factors, but it can be significantly higher than the pinhole duration for moderate to low stretch factors. As illustrated in Fig. 1, the uniform energy spectrum of the ideal incoherent-light source is practically realized over a limited frequency bandwidth. This imposes a limitation on the temporal aperture of the incoherent time-stretch system; i.e., the input RF signal to be processed must be within a temporal window

$$T_A = 2\pi|\ddot{\Phi}_1|\Delta f_{\text{opt}}, \tag{4}$$

where Δf_{opt} is the frequency bandwidth of the incoherent-light source. Thus, a large temporal aperture requires the use of a light source with an ultrabroad spectrum in such a way that the coherence time of the source is typically much shorter than the target temporal resolution and the related pinhole duration. As shown by Eqs. (3) and (4), the temporal aperture and temporal resolution are nearly independent. However, we should note that there is a certain design trade-off between the temporal aperture and the stretch factor as they both depend on the input dispersion amount in an inverse fashion.

3. Results

To demonstrate the introduced concept, we set up an incoherent time-stretch experiment, as illustrated in Fig. 2. Broadband incoherent light with a nearly uniform spectrum is first generated by filtering a superluminescent diode and then amplified by a semiconductor optical amplifier [8]. A broadband incoherent pulse is then obtained by sending the incoherent light through a temporal pinhole. The temporal pinhole here is realized by a 40 GHz electro-optic intensity modulator that is driven by a narrow electronic pulse generated by a 12 Gsamples/s AWG and amplified by a 12.5 GHz electronic amplifier. The broadband incoherent pulse is first amplified by an erbium-doped fiber amplifier (EDFA) and then dispersed by the first dispersive line, which induces an averaged linear

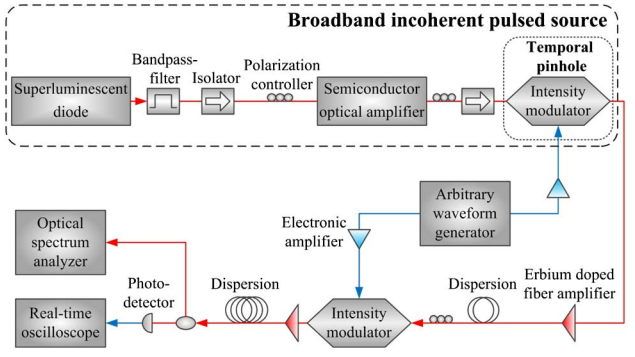

Fig. 2. Experimental setup of the incoherent time-stretch system.

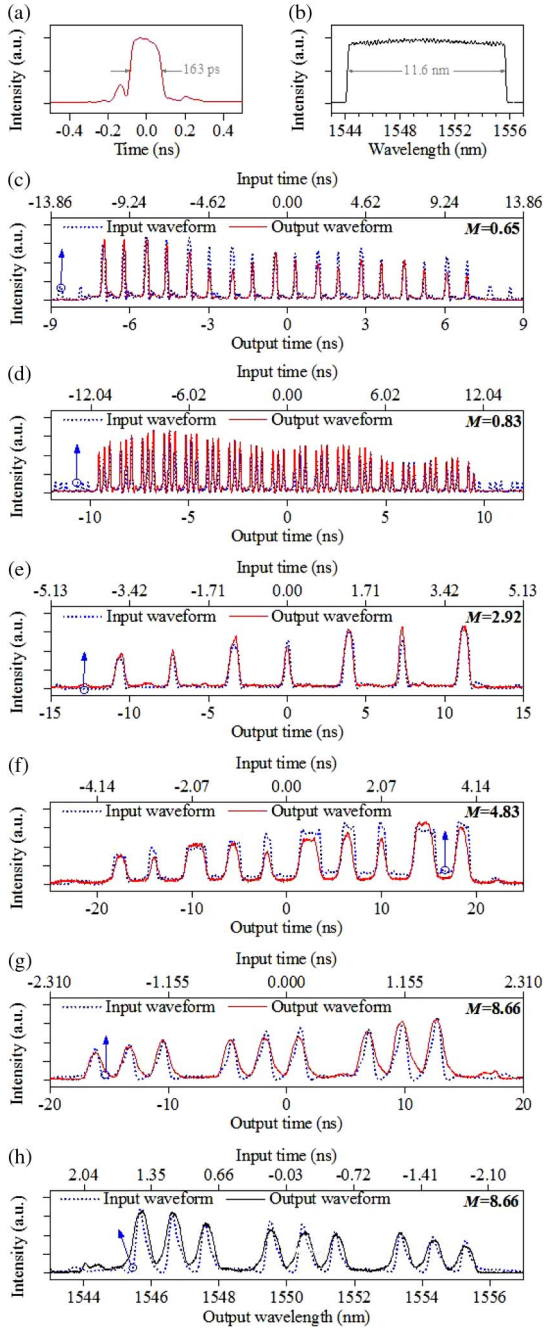

Fig. 3. Experimental demonstration of incoherent time stretch. (a) and (b) show the averaged temporal intensity profile and the averaged spectrum of the incoherent pulse at the output of the broadband incoherent pulsed source, respectively. Five experiments with different stretch factors M are shown in (c)–(g), respectively. In particular, the temporally stretched output waveforms (solid red) are compared with the scaled input waveforms (dotted blue), where the scaling factors in the figures are fixed to match the theoretical time-stretch factors. Additionally, the plots in (h) show the spectrum of the system output (solid black), compared with the scaled input temporal waveform (dotted blue), where the scaling factor in the figure is fixed according to the input dispersion value of –346 ps/nm. All profiles in (a)–(h) are averaged for 256 times.

Table 1. Performance Specifications for Experiments Shown in Fig. 3

Experiments	First Dispersion	Second Dispersion	Stretch Factor	Input Temporal Aperture	Input Temporal Resolution	TBP
Fig. 3(c)	1981 ps/nm	−692 ps/nm	0.65	~22.98 ns	~107.8 ps	~213.2
Fig. 3(d)	1981 ps/nm	−346 ps/nm	0.83	~22.98 ns	~67.5 ps	~340.4
Fig. 3(e)	−692 ps/nm	−1326 ps/nm	2.92	~8.03 ns	~85.3 ps	~94.1
Fig. 3(f)	−692 ps/nm	−2652 ps/nm	4.83	~8.03 ns	~123.4 ps	~65.1
Figs. 3(g) and 3(h)	−346 ps/nm	−2652 ps/nm	8.66	~4.02 ns	~122.7 ps	~32.8

frequency chirp. Subsequently, the input RF signal, which is generated by the same AWG and amplified by a 12 GHz electronic amplifier, is modulated onto the dispersed light using another 40 GHz electro-optic intensity modulator. Time-to-frequency mapping is achieved by the combination of linear frequency chirp and the second intensity modulation process. After that, the modulated light is amplified again and sent through the second dispersive line, which implements frequency-to-time mapping. The temporal intensity profile at the system output is measured with a 45 GHz photo-detector coupled to a 28 GHz electronic real-time oscilloscope, and the spectrum of the system output is measured by an optical spectrum analyzer with a resolution of 0.02 nm.

We report here results from five experiments with different time-stretch factors, including examples of temporal compression and magnification; see the results in Fig. 3. In these experiments, three different input temporal waveforms are used. In particular, Table 1 provides the values of the first and second dispersion used in these five experiments. Figures 3(a) and 3(b) show the averaged temporal intensity profile and the averaged spectrum of the incoherent pulse at the output of the broadband incoherent pulsed source, respectively. The time width (intensity FWHM) and bandwidth (intensity FWHM) of the incoherent pulse are 163 ps and 11.6 nm, respectively. The incoherent pulse has a duration that is nearly 360 times longer than the coherence time of the light source. As shown in Figs. 3(c)–3(g), the temporally stretched output waveforms (solid red, averaged for 256 times) closely resemble the corresponding scaled input waveforms (dotted blue). Note

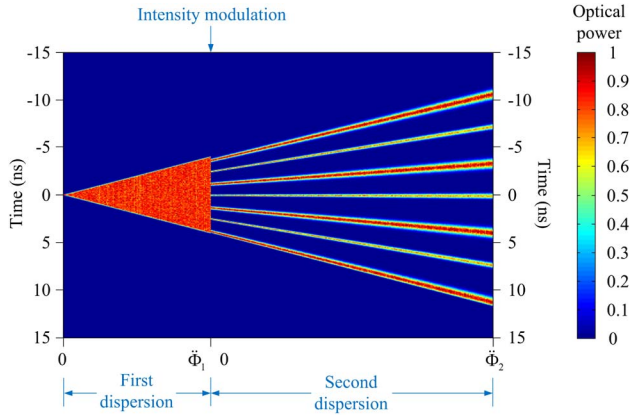

Fig. 4. Carpet for incoherent time stretch. The carpet illustrates the evolution of the signal along the system for the experimental result shown in Fig. 3(e).

that the input waveforms are averaged optical temporal intensity profiles measured at the output of the second intensity modulator. The small pulses in the input waveforms beyond the temporal aperture are due to the fact that the bias of the first intensity modulator (temporal pinhole) is not fully optimized. However, these pulses fall outside the system temporal aperture, and, thus, they are not observed in the corresponding output waveforms (particularly in Figs. 3(c) and 3(d)). To show the time-to-frequency mapping achieved at the output of the second intensity modulator, which is the first step of the incoherent time stretch, the measured spectrum at the system output (solid black) in the last experiment (which corresponds to Fig. 3(g)) is shown in Fig. 3(h). There is again an excellent agreement between the measured spectrum at the system output and the scaled input temporal waveform (dotted blue). Additionally, Fig. 4 illustrates the evolution of the signal along the time-stretch system for the experimental example shown in Fig. 3(e).

The performance specifications of the demonstrated systems are given in Table 1. The stretch factors and temporal apertures estimated from the experimental results are in excellent agreement with our theoretical predictions. In terms of temporal resolutions, they are essentially limited by the pinhole duration, as shown in Eq. (3), in such a way that the theoretical values for the input resolution in the reported experiments are 87.5, 34.5, 107.1, 129.3, and 144.2 ps, respectively. As shown in Table 1, the resolutions estimated from the obtained experimental results [8,9] are slightly deviated from these theoretical values. There are two reasons for the deviation. The first is that in the resolution estimation we have assumed the input pulses to be Gaussian-like, whereas the practical input pulses are slightly deviated from Gaussian pulses, as shown in Fig. 3. The second reason is due to the limiting bandwidth of the real-time oscilloscope.

4. Discussion and Conclusion

In summary, we have theoretically proposed and experimentally demonstrated a new time-stretch system based on an incoherent pulsed light source. The proposed incoherent scheme can provide similar performance specifications to those of its coherent counterpart but using a temporal gating process significantly longer than the transform-limited pulse duration of the equivalent coherent mode-locked laser system. However, implementation of incoherent-light photonic time stretch requires operation of the

oscilloscope in average mode, a fact that may preclude real-time operation. This drawback may be potentially overcome by using a suitable discrete-spectrum (multiwavelength) laser source, a strategy that has been demonstrated successfully for other incoherent-light temporal signal processing operations [10]. The novel concept proposed here could potentially be useful to improve many of the previous signal processing platforms based on coherent photonic time stretching of RF waveforms.

References

1. J. A. Wepman, "Analog-to-digital converters and their applications in radio receivers," IEEE Commun. Mag. **33**(5), 39–45 (1995).
2. R. H. Walden, "Analog-to-digital converter survey and analysis," IEEE J. Sel. Areas Commun. **17**, 539–550 (1999).
3. K. Goda and B. Jalali, "Dispersive Fourier transformation for fast continuous single-shot measurements," Nat. Photonics **7**, 102–112 (2013).
4. Y. Han and B. Jalali, "Photonic time-stretched analog-to-digital converter: fundamental concepts and practical considerations," J. Lightwave Technol. **21**, 3085–3103 (2003).
5. J. Azaña, N. K. Berger, B. Levit, and B. Fischer, "Broadband arbitrary waveform generation based on microwave frequency upshifting in optical fibers," J. Lightwave Technol. **24**, 2663–2675 (2006).
6. A. M. Fard, S. Gupta, and B. Jalali, "Photonic time-stretch digitizer and its extension to real-time spectroscopy and imaging," Laser Photon. Rev. **7**, 207–263 (2013).
7. D. Solli, C. Ropers, P. Koonath, and B. Jalali, "Optical rogue waves," Nature **450**, 1054–1057 (2007).
8. B. Li and J. Azaña, "Incoherent-light temporal stretching of high-speed intensity waveforms," Opt. Lett. **39**, 4243–4246 (2014).
9. M. A. Foster, R. Salem, D. F. Geraghty, A. C. Turner-Foster, M. Lipson, and A. L. Gaeta, "Silicon-chip-based ultrafast optical oscilloscope," Nature **456**, 81–84 (2008).
10. A. Malacarne, R. Ashrafi, M. Li, S. LaRochelle, J. Yao, and J. Azaña, "Single-shot photonic time-intensity integration based on a time-spectrum convolution system," Opt. Lett. **37**, 1355–1357 (2012).